Electronic Supplementary Material (ESI) for Nanoscale Advances.
This journal is © The Royal Society of Chemistry 2021

Supplementary Information

MC_2 (M = Y, Zr, Nb, and Mo) Monolayers Containing C_2 Dimers: Prediction of Anode Materials for High-performance Sodium Ion Batteries

Zhanzhe Xu[1], Xiaodong Lv[2,3,4]*, Wenyue Gu[1], Fengyu Li[1,]*

[1] *School of Physical Science and Technology, Inner Mongolia University, Hohhot, 010021, China*

[2] *CAS Key Laboratory of Magnetic Materials and Devices, Ningbo Institute of Materials Technology and Engineering, Chinese Academy of Sciences, Ningbo 315201, China.*

[3] *Zhejiang Province Key Laboratory of Magnetic Materials and Application Technology, Ningbo Institute of Materials Technology and Engineering, Chinese Academy of Sciences, Ningbo 315201, China.*

[4] *Ganjiang Innovation Academy, Chinese Academy of Sciences, Ganzhou 341000, People's Republic of China.*

*Corresponding authors: lvxiaodong@nimte.ac.cn (XL); fengyuli@imu.edu.cn (FL)

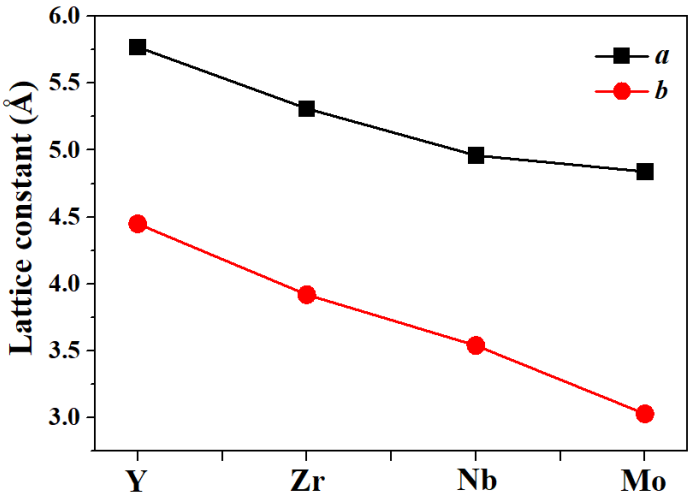

Fig. S1 Lattice constants (*a*, *b*) of the MC_2 (M = Y, Zr, Nb and Mo) monolayers.

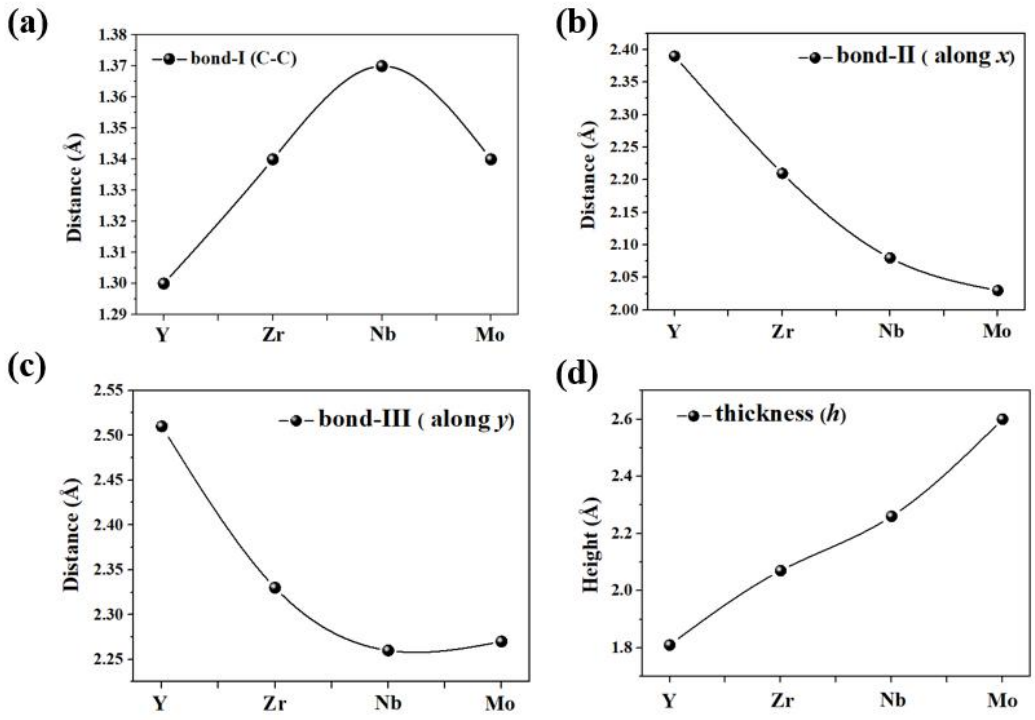

Fig. S2 Bonds length of C−C (a), M−C in the (b) (c) and thickness (*d*) for the MC_2 (M = Y, Zr, Nb and Mo) monolayers.

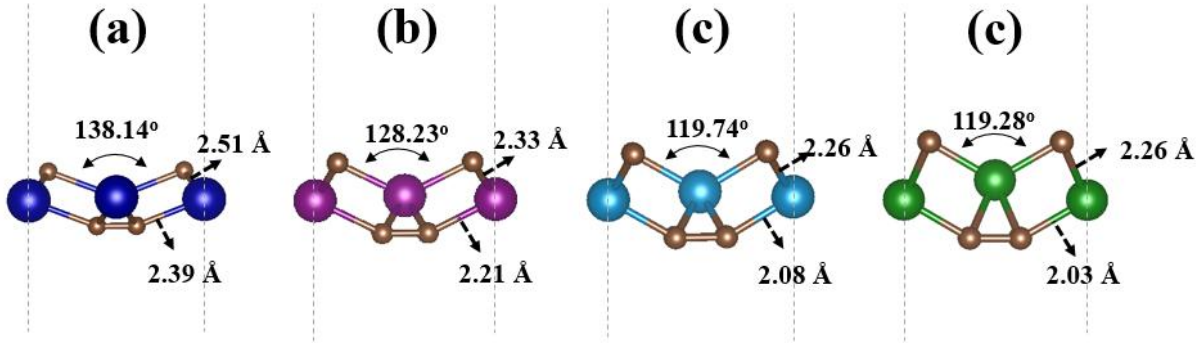

Fig. S3 Bonds length of M−C along the *x* (*y*)-direction and bond angel (□ □C-M-C) for the MC_2 (a) YC_2; (b) ZrC_2; (c) NbC_2 and (d) MoC_2 monolayers.

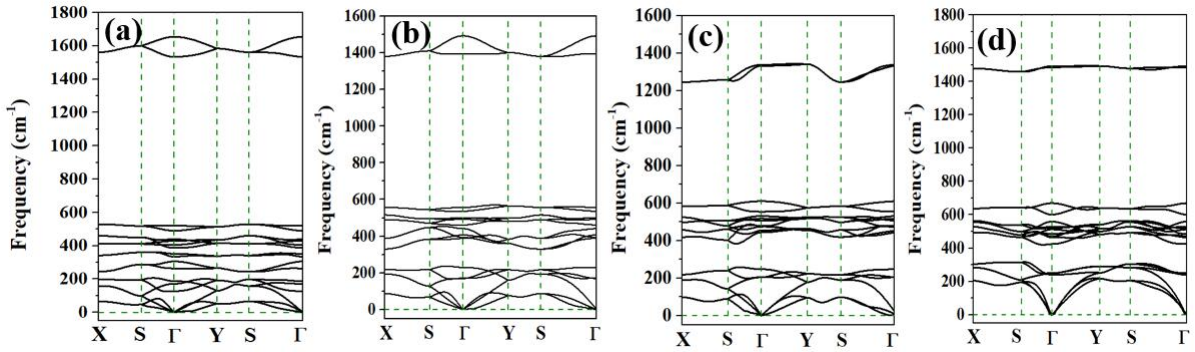

Fig. S4 The calculated phonon spectra of the YC_2 (a), ZrC_2 (b), NbC_2 (c), and MoC_2 (d) monolayers.

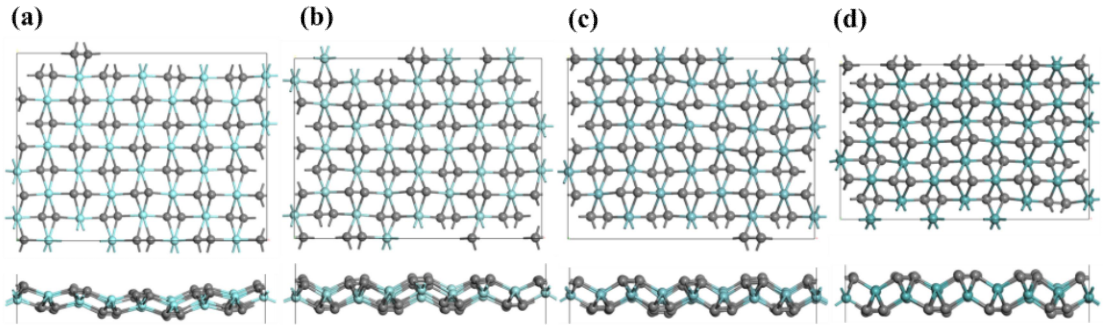

Fig. S5 The snapshots of the YC_2 (a), ZrC_2 (b), NbC_2 (c) and MoC_2 (d) monolayers at the end of 5 ps FPMD simulations at 300 K.

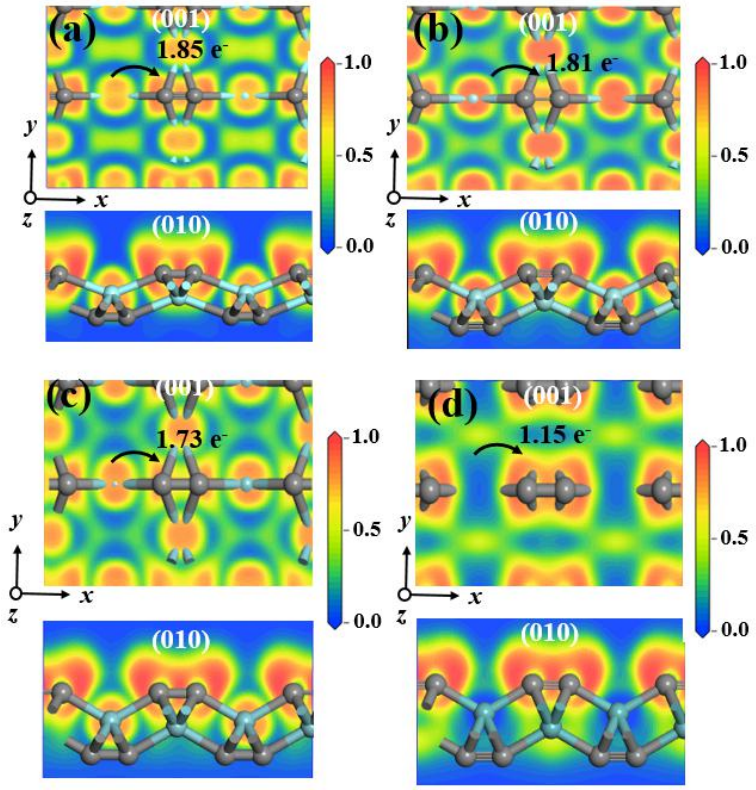

Fig. S6 The electronic localization function (ELF) of the YC_2 (a), ZrC_2 (b), NbC_2 (c) and MoC_2 (d) monolayers. In the ELF maps, the red and blue colors refer to the highest value (1.00) and the lowest value (0.00) of ELF, respectively. Corresponding to the accumulation and depletion of electrons in the two colored regions.

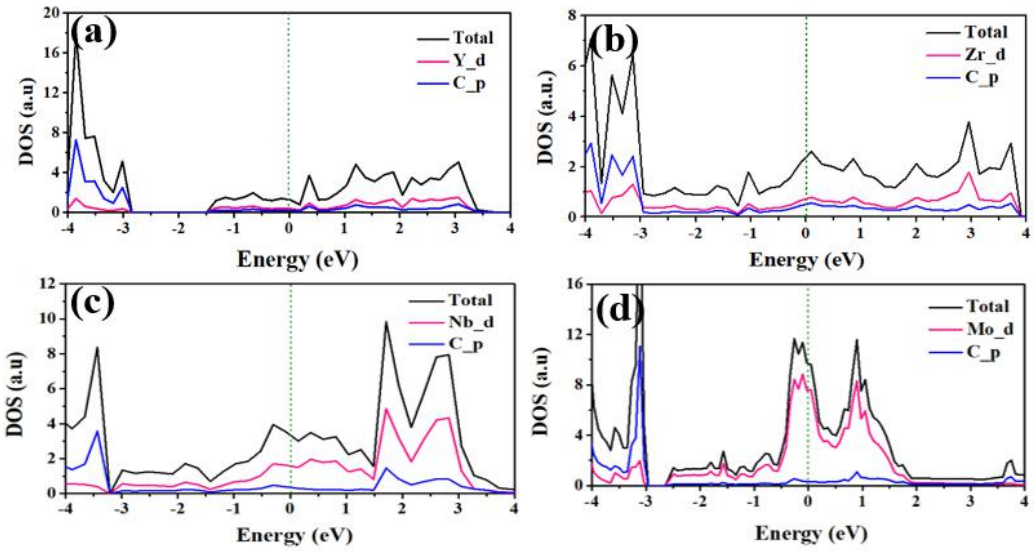

Fig. S7 The partial density of states of the YC_2 (a), ZrC_2 (b), NbC_2 (c), and MoC_2 (d) monolayers. The Fermi energy is set to 0 eV as indicated by the vertical dashed line.

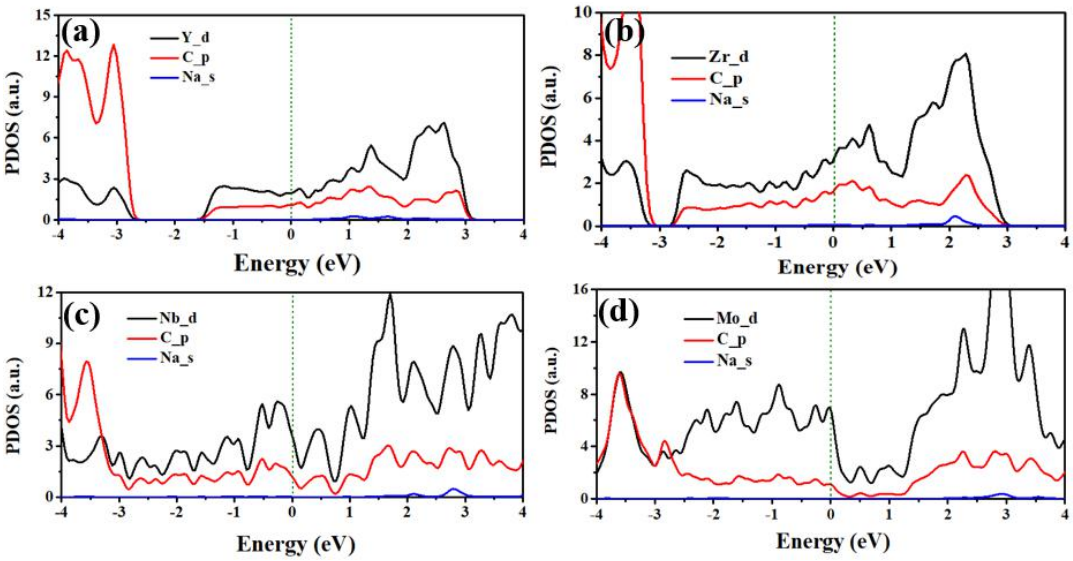

Fig. S8 The partial density of states of Na-adsorbed YC_2 (a), ZrC_2 (b), NbC_2 (c), and MoC_2 (d) monolayers. The Fermi energy is set to 0 eV as indicated by the vertical dashed line.

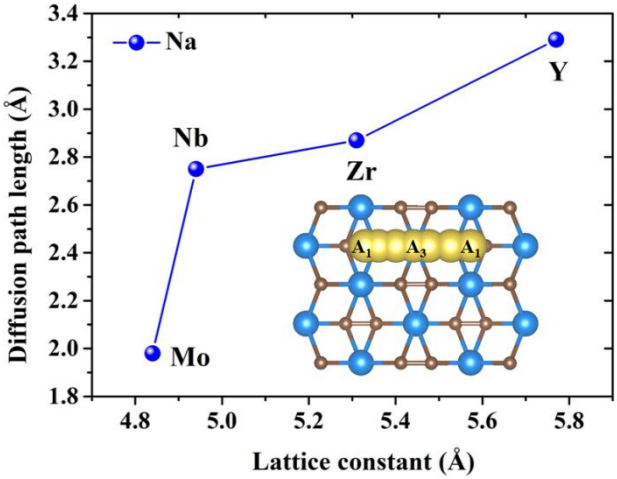

Fig. S9 The variation of Path-I diffusion lengths of Na on the MC_2 (M = Y, Zr, Nb, and Mo) monolayers with the lattice constants of MC_2.

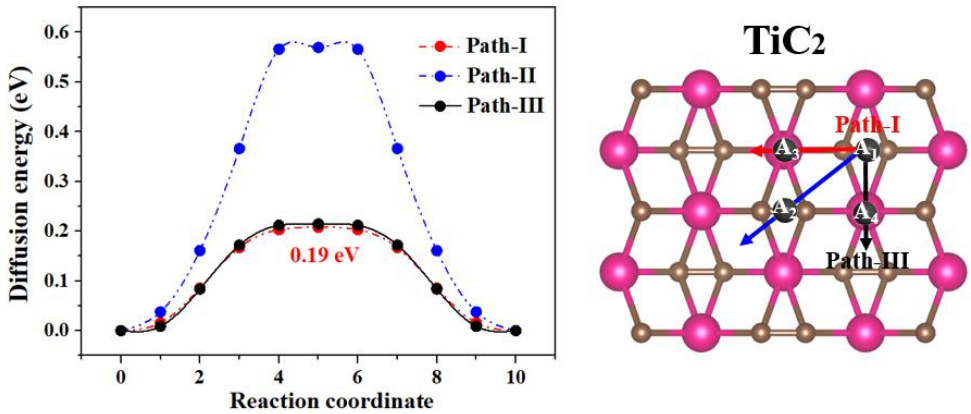

Fig. S10 The energy profile (left) and diffusion pathways (right) of Na diffusing on the TiC_2 monolayer.

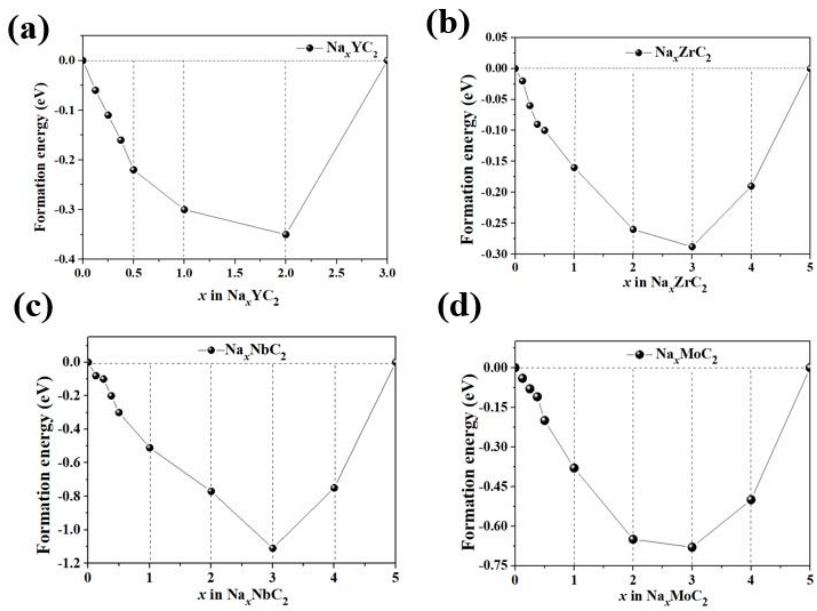

Fig. S11 The formation energy (E_f) of Na_xYC_2 (a), Na_xZrC_2 (b), Na_xNbC_2 (c), and Na_xMoC_2 (d) with respect to MC_2 monolayer and Na bulk *bcc* metal. Data points located on the convex hull represents the stable adsorption without decomposition.

Here, the most stable adsorptions configuration of different Na adsorption concentrations (x) on the MC_2 monolayer, we calculated the based on the following equation:[S1]

$$E_f(x) = (E_{NaxMC2} - E_{MC2} - xE_{Na\text{-}bulk})/(x+1) \qquad (1)$$

where E_{MC2}, E_{NaxMC2}, and $E_{Na\text{-}bulk}$ are the energy of MC_2 monolayer, the total energy of Na-adsorbed MC_2, and the energy per atom in the bulk Na, respectively. We plotted the convex energy hull, the cure of formation energies of all configurations considered *vs.* the concentrations of Na (x) in the intercalated MC_2 systems. Located on the hull with negative formation energies, and thus thermodynamically stable, these data further confirm the stability of Na_2YC_2, Na_3ZrC_2, Na_3NbC_2, and Na_3MoC_2.

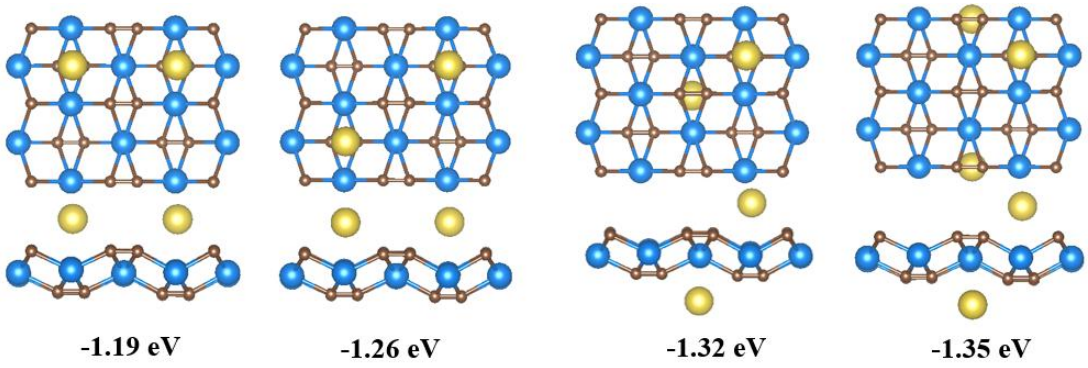

Fig. S12 The optimized configurations and the corresponding average adsorption energies of Na for $Na_{0.25}NbC_2$.

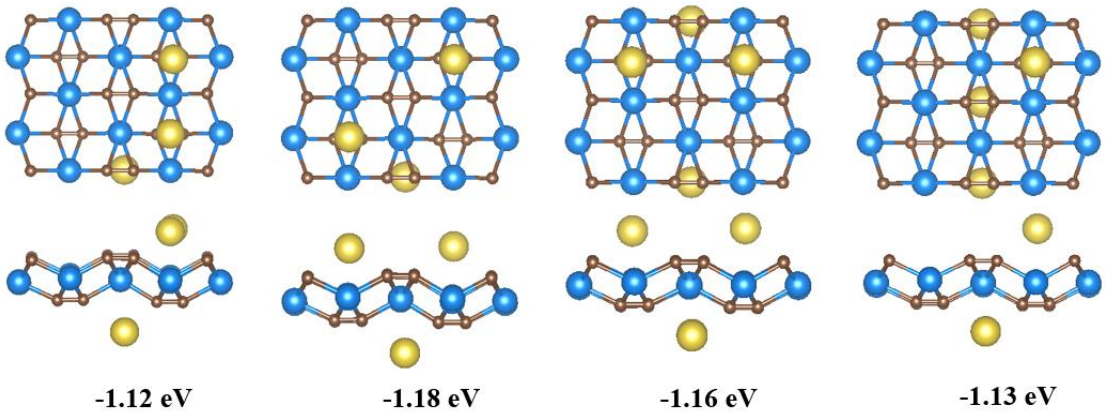

Fig. S13 The optimized configurations and the corresponding average adsorption energies of Na for $Na_{0.375}NbC_2$.

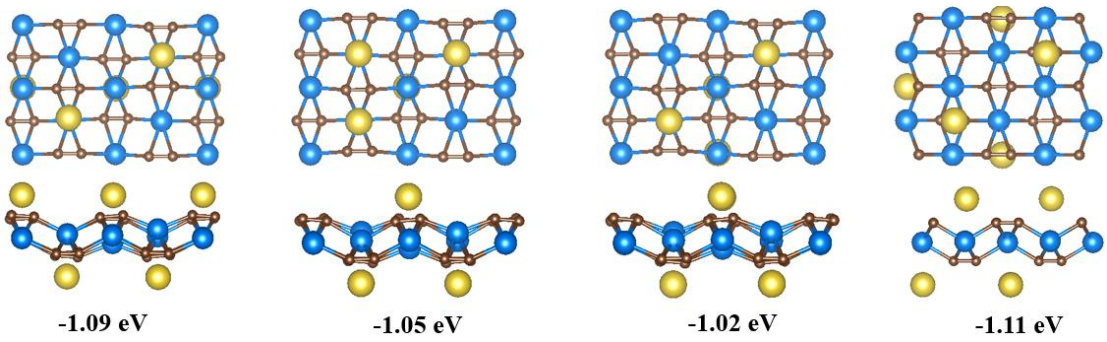

Fig. S14 The optimized configurations and the corresponding average adsorption energies of Na for $Na_{0.5}NbC_2$.

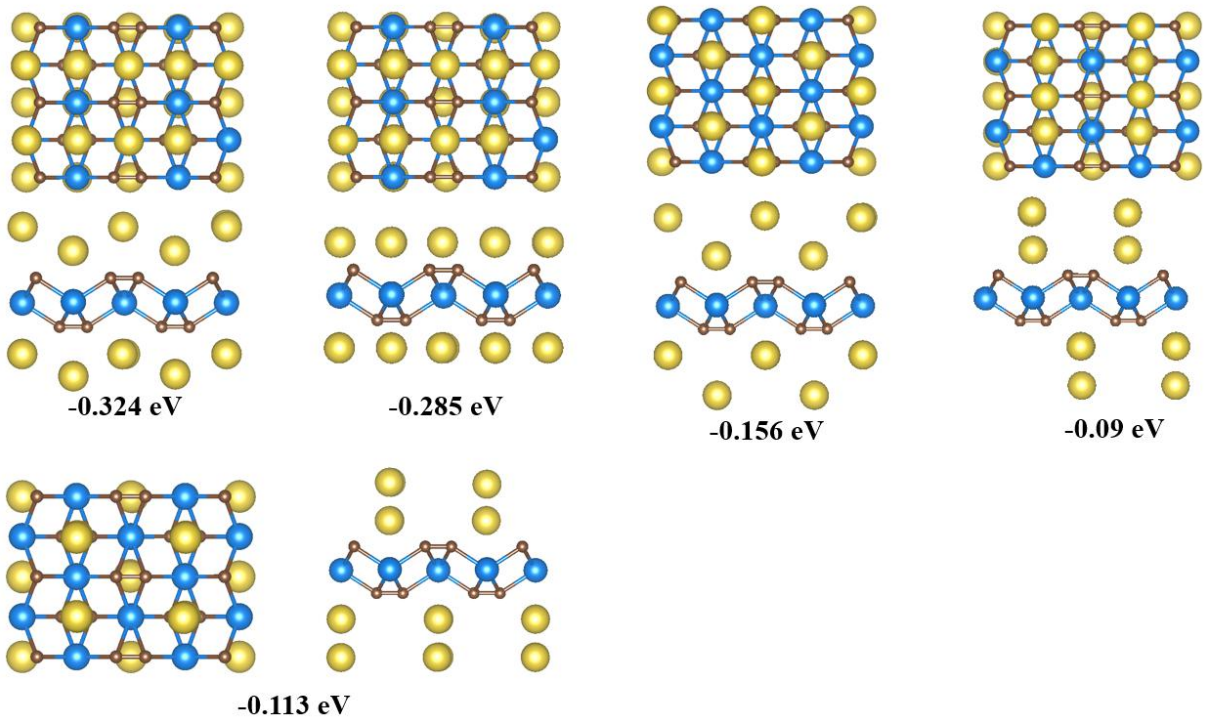

Fig. S15 The optimized configurations and the average adsorption energies of Na for Na_2NbC_2: the additional 8 Na all adsorb at the A_3 sites more far to the surface (E_{ave} = -0.324 eV), the additional 8 Na all adsorb at the A_3 sites with the same height to the surface of the preadsorbed Na at A_1 sites (E_{ave} = -0.285 eV), the additional 8 Na all adsorb at the A_3 sites more far to the surface (E_{ave} = -0.324 eV), the additional 8 Na all adsorb at the A_1 sites more far to the surface (E_{ave} = -0.156 eV), the additional 8 Na all adsorb at the A_4 sites more far to the surface (E_{ave} = -0.009 eV), the additional 8 Na all adsorb at the A_2 sites more far to the surface (E_{ave} = -0.113 eV).

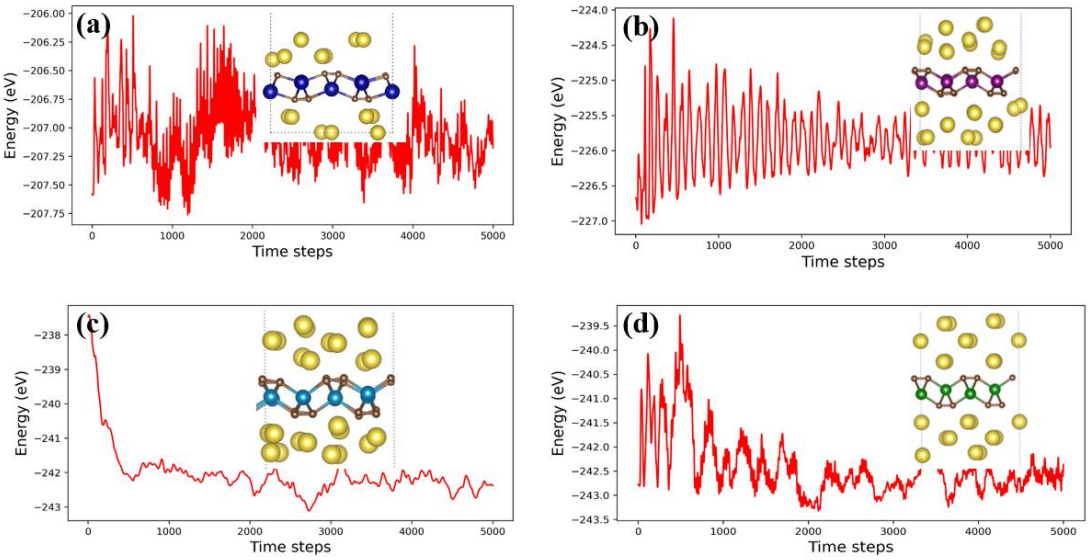

Fig. S16 The end structures (side view) of the Na-intercalated MC_2 (M = Y, Zr, Nb, and Mo) monolayers through a 5 ps FPMD simulation at 300 K.

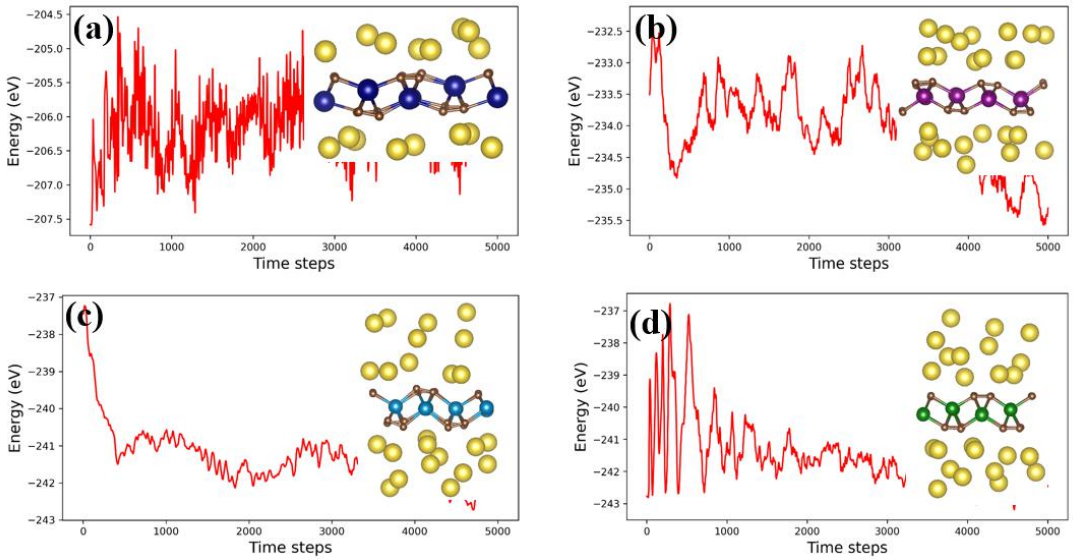

Fig. S17 The end structures (side view) of the Na-intercalated MC_2 (M = Y, Zr, Nb, and Mo) monolayers through a 5 ps FPMD simulation at 500 K.

Table S1. The calculated lattice constant (*a*, *b*, Å), lattice and volume change of MC_2 (M = Y, Zr, Nb, and Mo) nanosheets without and with adsorbed Na atoms.

	a **(Å)**	***b*** **(Å)**	**Lattice variation (%)**		**Volume variation (%)**
YC_2	11.60	8.56			
Na_2YC_2	11.84	8.10	2.1	-5.3	9.8
ZrC_2	10.67	7.78			
Na_3ZrC_2	10.73	7.19	0.5	-7.5	0.8
NbC_2	9.95	7.10			
Na_3NbC_2	9.77	6.70	-1.8	-5.6	6.9
MoC_2	9.68	6.02			
Na_3MoC_2	9.56	6.18	-1.2	2.6	6.05

[S1] (a) T. Bo, P. F. Liu, J. Xu, J. R. Zhong, Y. B. Chen, O. Eriksson, F. W. Wang and B. T. Wang, *Phys. Chem. Chem. Phys*., 2018, **20**, 22168–22178; (b) T. Bo, P. F. Liu, J. Xu, J. R. Zhong, F. W. Wang and B. T. Wang, *Phys. Chem. Chem. Phys*., 2019, **21**, 5178–5188.